Aeronautical Research Institute, University of Tokyo
Report No. 375, November 1962

Boundary-Layer Transition by Isolated Roughness

By

Itiro TANI, Hiroyuki KOMODA*, Yasuo KOMATSU*
and Matsusaburo IUCHI

Summary. Results of hot-wire measurements are presented on transition in laminar boundary layer along a flat plate with zero pressure gradient in the presence of an isolated roughness element. Transition occurs in the region of a wedge whose vertex moves rapidly forward with slightest increase in stream velocity or roughness height until finally it reaches the roughness element. The critical condition that just causes a wedge of turbulence to originate from roughness is governed by a critical value of the roughness Reynolds number R_k, which is based on the roughness height and the velocity in the laminar boundary layer at the height of roughness. The critical value of R_k is a slowly decreasing function of the transition Reynolds number R_t, based on the free-stream velocity and the distance from leading edge to roughness location.

The spanwise distribution of mean velocity in the boundary layer behind a roughness element for subcritical values of R_k is indicative of the presence of streamwise vortices as first observed by Gregory and Walker. Except for the station close behind roughness, a horseshoe-shaped vortex wrapped round the front of roughness gives a predominant effect on mean velocity distribution, producing a primary peak behind the centerline of roughness, and a valley and a secondary peak outside. This three-dimensional deformation of mean velocity field is considered to account for the critical behavior of transition movement. Controlled two-dimensional disturbances created by a vibrating ribbon develop downstream in a way respectively characteristic of the central peak section, valley sectoin and outside peak section. The disturbances are most strongly amplified in the outside peak section, until breakdown of laminar flow takes place at a downstream station. This breakdown corresponds to the beginning of a turbulent wedge at that station.

INTRODUCTION

It has been known since the thirties that a dirt particle or similar isolated roughness on the surface in the region of laminar flow may produce immediate transition, a wedge-shaped region of turbulent flow originating at the roughness and extending downstream. It has also been observed that when stream velocity or roughness height is reduced, the wedge of turbulence may begin some distance downstream from the roughness element.

Gregory and Walker [*1*] appear to have been the first to make systematic investigations of this type of transition. They observed under certain conditions the china-clay records of twin streaks suggestive of vortex filaments in the boundary layer downstream of the roughness, ultimately disintegrating into a wedge of turbulence. Closer examination by smoke revealed a horseshoe-shaped vortex

* Department of Mechanical Engineering, Nihon University

wrapped round the front of the roughness and trailing downstream. The slightest increase in stream velocity or roughness height changed the pattern from twin streaks to a fully turbulent wedge originating at the roughness element. This quick movement of transition position seems to distinguish the effect of three-dimensional roughness from that of two-dimensional roughness, for which transition moves rather gradually forward as the stream velocity is increased.

It is now known through the investigations of Fales [*3*], Weske [*5*], Hama, Long and Hegarty [*6*], and Schubauer [*7*] that a two-dimensional roughness element produces two-dimensional disturbances which develop into three-dimensional configuration before eventually disintegrating into turbulence. Formation of three-dimensional disturbances is considered a prerequisite to turbulence, and this explains the gradual approach of transition with the increase in stream velocity. On the other hand, a three-dimensional roughness element is more straightforward in producing three-dimensional disturbances, thus effecting transition to move quickly forward as soon as the critical velocity is reached.

The critical stream velocity or roughness height that just causes a wedge of turbulence to spread from roughness seems to be governed by a fixed value of the roughness Reynolds number, which is based on the roughness height and the velocity in the laminar boundary layer at the height of roughness element. A critical value of 440 was suggested for this roughness Reynolds number by Klanfer and Owen [*2*], who reanalyzed Gregory and Walker's data for conical roughness on airfoils having zero or slightly favorable pressure gradients. Subsequent measurements of Klebanoff, Schubauer and Tidstrom [*4*] for spherical roughness on a flat plate with zero pressure gradient gave a critical value ranging from 500 to 800, but a proper comparison would be difficult in view of the differences between the two experiments, especially in regard to the type of roughness, turbulence and pressure gradient of the stream, and the definition of the critical roughness Reynolds number.

The paper presents results of experimental investigation on the effect of an isolated roughness element on a flat plate with zero pressure gradient. The investigation aimed first at determining the critical roughness Reynolds number in an extensive range of parameters, and second at exploring the flow patterns behind roughness element to elucidate the critical nature of transition. Brief accounts concerning the first and second problems have already been published by Tani in the "Boundary Layer and Flow Control", Pergamon Press 1961 [*8*], and at the Third Congress of International Council of the Aeronautical Sciences, Stockholm 1962 [*13*], respectively. The authors take this opportunity to express their thanks for helpful discussions to the members of Boundary Layer Research Group, with its center in the Aeronautical Research Institute, and for efficient assistance in experiments to Mr. Satoru Akiyama and Miss Naoko Handa of Nihon University, and Mr. Isamu Shimizu of Aeronautical Research Institute.

Experimental Arrangements

Most of the measurements were made on the boundary layer along an aluminum flat plate, 300 cm long, 60 cm wide and 0.5 cm thick, with a sharpened leading edge. The plate was mounted in the wind tunnel LT-1 having 20 cm by 60 cm working section. The tunnel wall was adjusted to give zero pressure gradient along the plate. Results presented were obtained at free-stream velocity U_0 of 3 to 15 m/s. The free-stream turbulence level was about 0.05 per cent at $U_0 = 10$m/s. The reference axes were taken in such a way that x was measured along the plate from the leading edge in the streamwise direction, y in the direction perpendicular to the plate, and z in the spanwise direction perpendicular to x and y.

Additional measurements were also made on a flat plate mounted in another wind tunnel N-1 having 60 cm by 60 cm working section, in which the turbulence level was about 0.2 per cent at a free-stream velocity of 5 m/s.

An isolated roughness element was represented by a single cylinder placed with its axis in y direction centrally on the flat plate at a location $x = x_k$, $z = 0$. The height k of the cylinder was equal to its diameter.

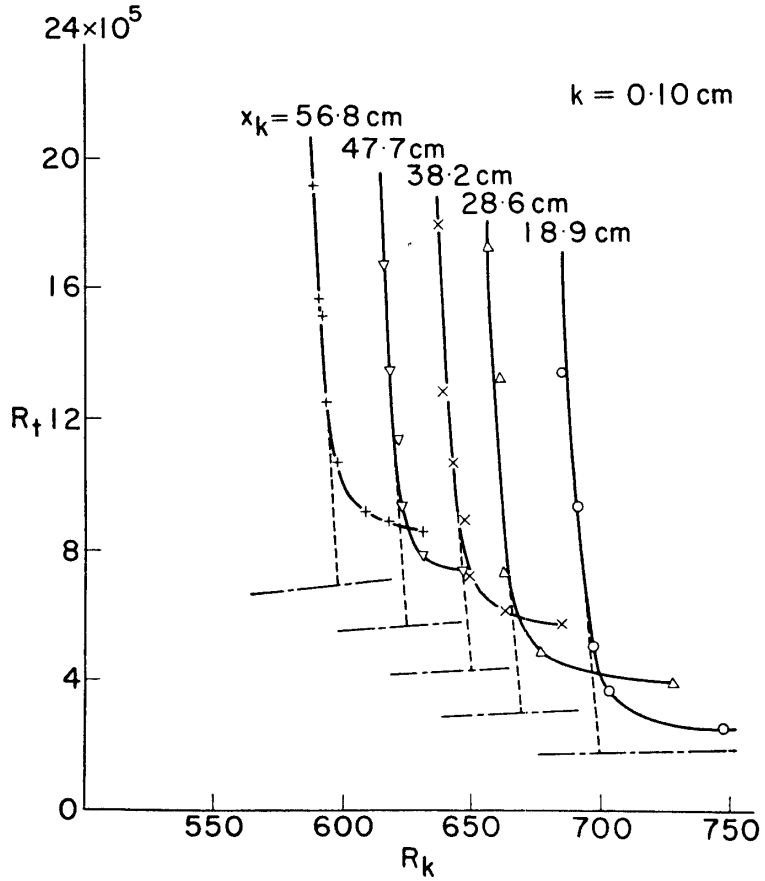

FIGURE 1. Variation of transition Reynolds number with roughness Reynolds number. Roughness height 0.10 cm. Wind tunnel LT-1.

Critical Roughness Reynolds Number

Consider a roughness element of height k is placed on the flat plate at a distance x_k from the leading edge at a free-stream velocity U_0. It is assumed that the roughness is located ahead of the transition position, x_{t_0}, on a smooth plate. Transition to turbulent flow occurs in the region of a detached wedge with vertex at a location x_t provided $x_k < x_t < x_{t_0}$. With the slightest increase in U_0, x_t approaches x_k until eventually the wedge is attached to the roughness element $(x_t = x_k)$.

The transition position x_t was determined by traversing a hot-wire probe along the centerline downstream from the roughness element $(z=0)$, and locating the point where the velocity fluctuation had an intermittency factor of 50 per cent. Typical results of measurements are shown in Figure 1, in which the transition Reynolds number $R_t = U_0 x_t/\nu$ is plotted against the roughness Reynolds number $R_k = k u_k/\nu$, u_k being the velocity in the laminar boundary layer at the height of roughness element and calculated by the formula $u_k = 0.332\, k U_0 (U_0/\nu x_k)^{\frac{1}{2}}$. The curve corresponding to the limiting case $x_t = x_k$ is given by $R_t = 2.08 (x_k/k)^{\frac{4}{3}} R_k^{\frac{2}{3}}$,

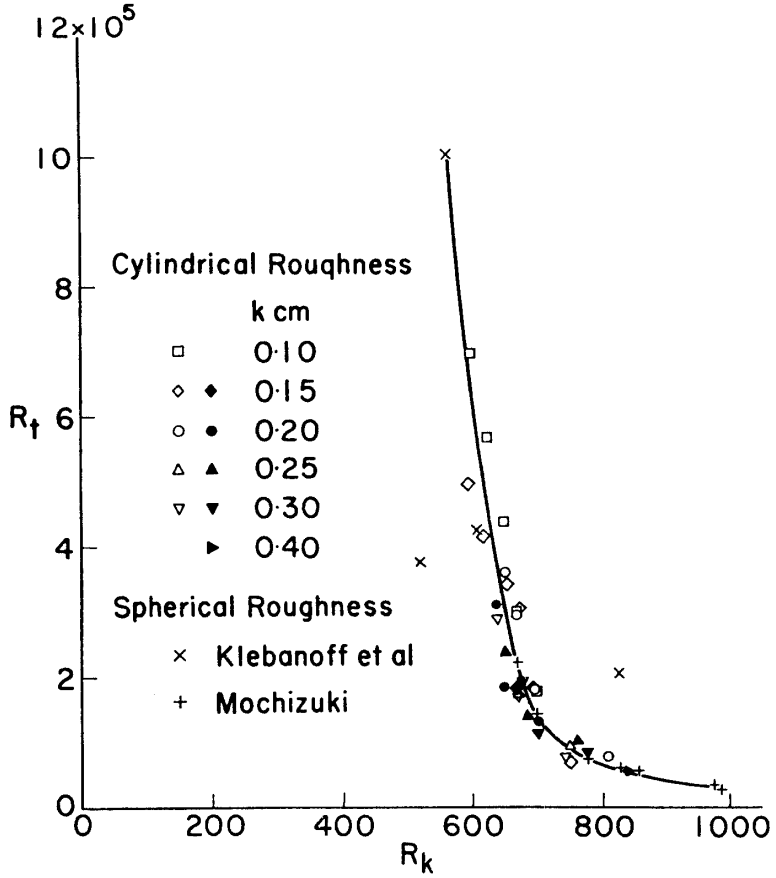

FIGURE 2. Variation of transition Reynolds number with critical roughness Reynolds number. Open and solid symbols (squares, circles and triangles) denote results for cylindrical roughness tested in wind tunnels LT-1 and N-1, respectively. Cross symbols denote results for spherical roughness from references 4 and 9.

and shown by chain line in Figure 1. The critical condition under which a wedge of turbulence just begins to spread from the roughness element can be determined by finding the extrapolated intersection with the limiting curve as indicated in Figure 1.

Results obtained in this way are collected in Figure 2, in which the transition Reynolds number R_t is plotted against the roughness Reynolds number R_k for the critical condition. Open and solid symbols (squares, circles and triangles) denote the points for which the free-stream turbulence levels are 0.05 and 0.2 per cent, respectively. In the figure are also included results deduced in a similar way by Klebanoff, Schubauer and Tidstrom [*4*] on spherical roughness elements in a spanwise row, and results obtained by smoke observation by Mochizuki [*9*] on a single spherical roughness element. It can be seen that the critical roughness Reynolds number is not constant but increases slightly as the transition Reynolds number is reduced. The increase of R_k in the lower range of R_t is apparently associated with the stability of the laminar boundary layer, for which the theoretical critical Reynolds number for stability against small disturbances is 6×10^4. It is rather remarkable to find the critical roughness Reynolds number lying in a narrow range, namely from 600 to 1000. Differences in free-stream turbulence scarcely affect the critical value. Additional measurements carried out on the cylindrical roughness elements in a spanwise row detected only a slight decrease in critical roughness Reynolds number from that of a single roughness element provided the spacing was larger than six times the roughness height. The effect of pressure gradient was also found small as regards the critical roughness Reynolds number.

Flow Field Behind Roughness Element

According to the visual observations, first carried out by Gregory and Walker [*1*] and recently elaborately extended by Mochizuki [*9*] [*10*], there exist two sets of streamwise vortices in the wake of a roughness element at roughness Reynolds number below its critical value. The one is a horseshoe-shaped vortex, wrapped round the front of the roughness. This can be traced back to the secondary flow in the boundary layer upstream of the roughness. The other is a pair of closely spaced vortex filaments originating from spiral filaments which rise vertically from points on the plate right behind the roghness element. These filaments are at about the level of the top of roughness element, while the horseshoe vortex is located close to the plate. The sense of rotation is such that momentum is to be transported downward (towards the plate) or upward by means of the horseshoe vortex and the closely spaced vortex filaments, respectively.

From these observations, however, it is not clear what effect these vortices have on the mechanism of transition. Their obvious effect is to redistribute momentum so that distortion in mean velocity field is expected to appear in the boundary layer downstream of the roughness element. Hot-wire measurements were therefore made in the wind tunnel N-1 to detect the spanwise variation of mean velocity.

Figure 3 shows the spanwise distributions of streamwise component of mean

velocity, U, and mean inclination of flow in xz plane, β, obtained by traversing two hot-wire probes in z direction at a fixed height y above the plate at a distance of 10 roughness heights from the roughness element. Distribution across the boundary layer of the velocity difference between peak and valley, U_1-U_2, is also shown

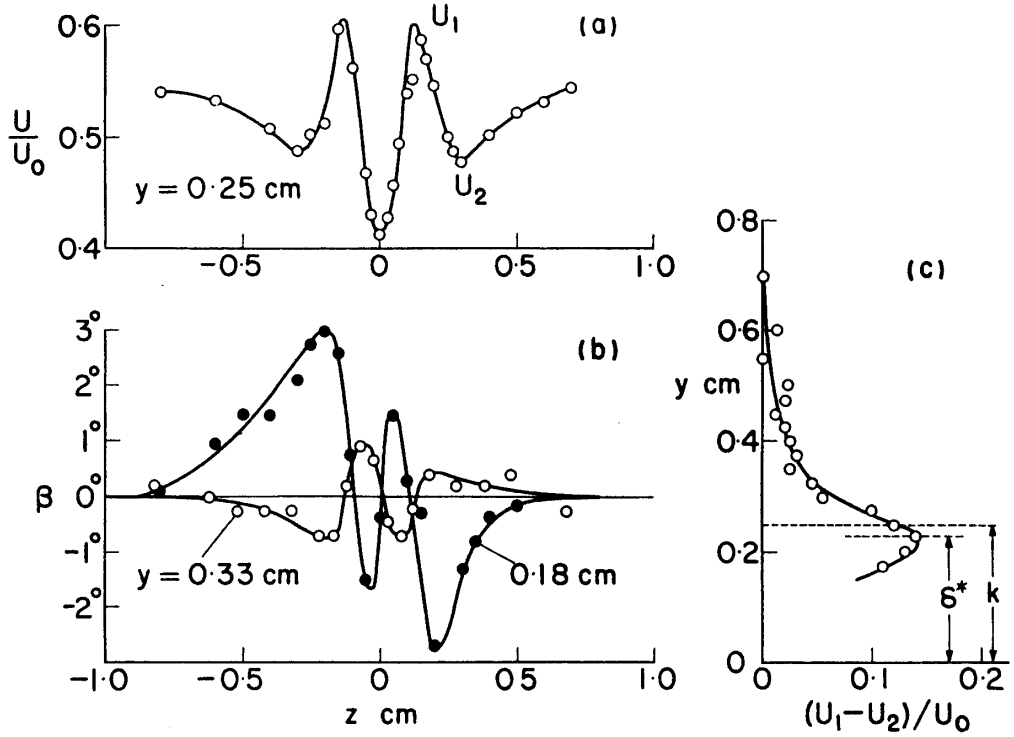

FIGURE 3. Spanwise distribution of (a) mean velocity and (b) flow inclination in xz plane at a fixed height above the flat plate. (c) Distribution across boundary layer of velocity difference between peak and valley. Roughness height k=0.25 cm, roughness location x_k=60 cm, distance from roughness $x-x_k$=2.5 cm, displacement thickness δ^*=0.23 cm, free-stream velocity U_0=5.2 m/s. Wind tunnel N-1.

in the figure. These distributions are clearly indicative of the existence of the two sets of vortices mentioned above.

Figure 4 shows the spanwise distribution of U observed at a distance of 244 roughness heights from the roughness element. Disappearance of double peaks in mean velocity distribution suggests the decay of the closely spaced vortex filaments at this downstream station. No noticeable inclination of flow could be detected.

It is to be noticed, however, that the effect of the horseshoe vortex, as judged from the velocity difference U_1-U_2, is only slightly reduced even at such a distance downstream. This is also shown in Figure 5, in which s/k and $(U_1-U_2)_{max}/U_0$ are plotted against $(x-x_k)/k$, s being the measure of spacing of horseshoe vortex defined by the distance between the two points having a velocity of $\frac{1}{2}(U_1+U_2)$. The indication is that no appreciable change occurs either in the spacing of or in the maximum velocity difference induced by the horseshoe vortex in the course of downstream development.

After these exploratory measurements in the wind tunnel N-1, more extensive measurements were made on a flat plate in the wind tunnel LT-1 by not only

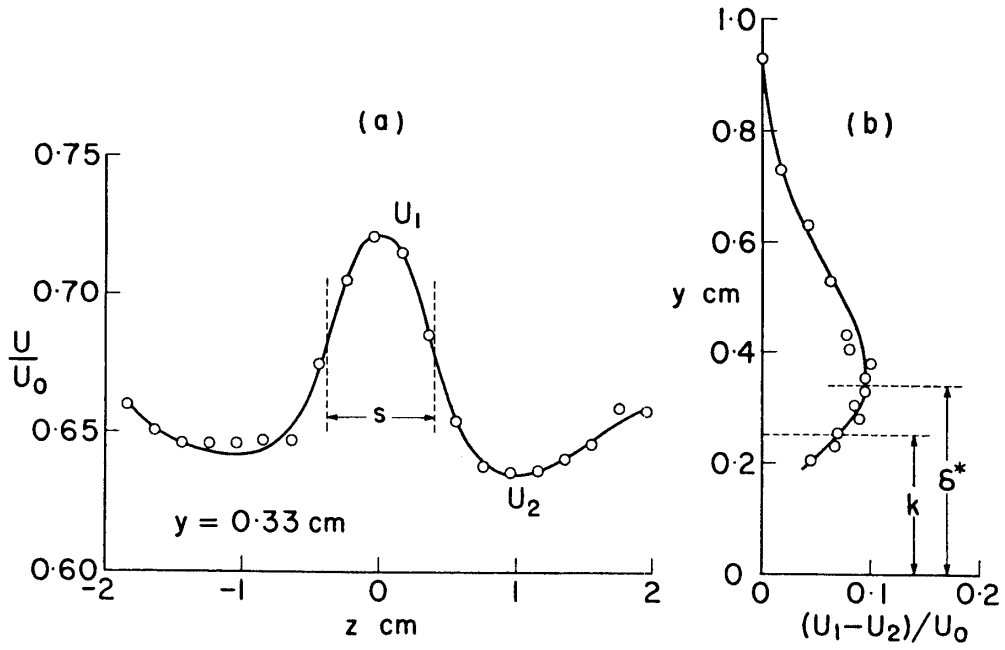

FIGURE 4. (a) Spanwise distribution of mean velocity at a height of 0.33 cm above flat plate. (b) Distribution across boundary layer of velocity difference between peak and valley. Roughness height $k=0.25$ cm, roughness location $x_k=60$ cm, distance from roughness $x-x_k=61$ cm, displacement thickness $\delta^*=0.34$ cm, free-stream velocity $U_0=5.2$ m/s. Wind tunnel N-1.

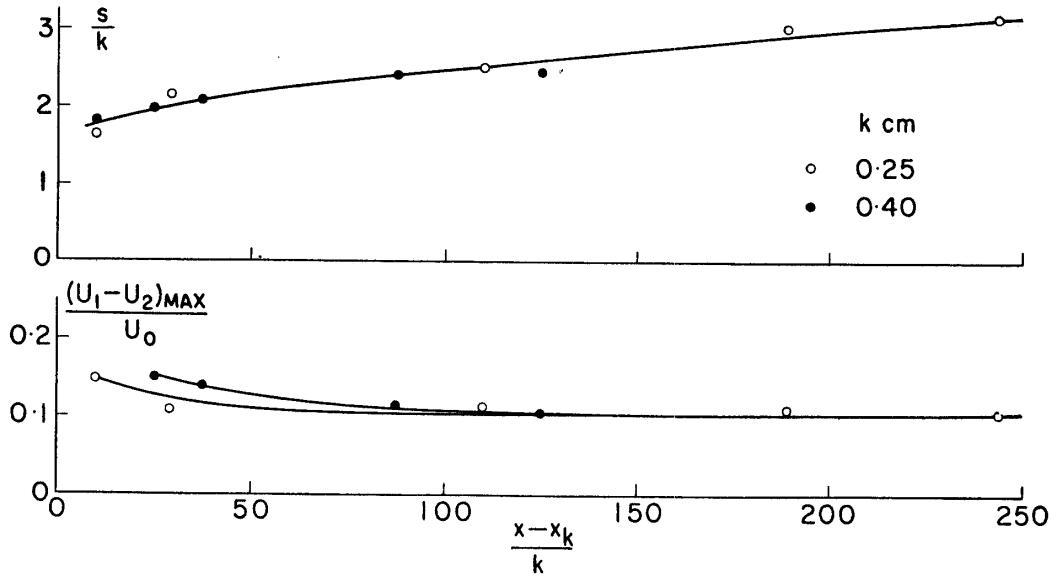

FIGURE 5. Variation in streamwise direction of spacing of and maximam velocity difference induced by horseshoe vortex. Roughness height $k=0.25$ and 0.40 cm, roughness location $x_k=60$ cm, free-stream velocity $U_0=5.2$ m/s. Wind tunnel N-1.

determining the distribution of mean velocity but also tracing the downstream development of controlled disturbances produced by Schubauer's technique of vibrating ribbon. A cylindrical roughness of 0.2-cm diameter and 0.2-cm height was placed on the plate at a distance $x_k=40$ cm from the leading edge. The free-stream velocity of $U_0=6.6$m/s was selected in such a way that the turbulent wedge began at a considerable distance from the roughness element but could be moved forward by passing a current through the vibrating ribbon. Results obtained with no current to vibrating ribbon are pressented in Figure 6, which shows the spanwise distribution of mean velocity U at a fixed height above the plate at various distances $x-x_k$ from the roughness element. Measurements were made at such a great distance from roughness that only the effect of horseshoe vortex was perceivable. As already mentioned in connection with Figure 5, the distance between valleys, and also that between outside peaks, of velocity variation remain almost unchanged in downstream development. For later reference, the sections for the central peak, the valled and the outside peak are denoted by A, E and F, respectively. The velocity distribution across the boundary layer in these sections were found to agree with the Blasius profile within the accuracy of measurements.

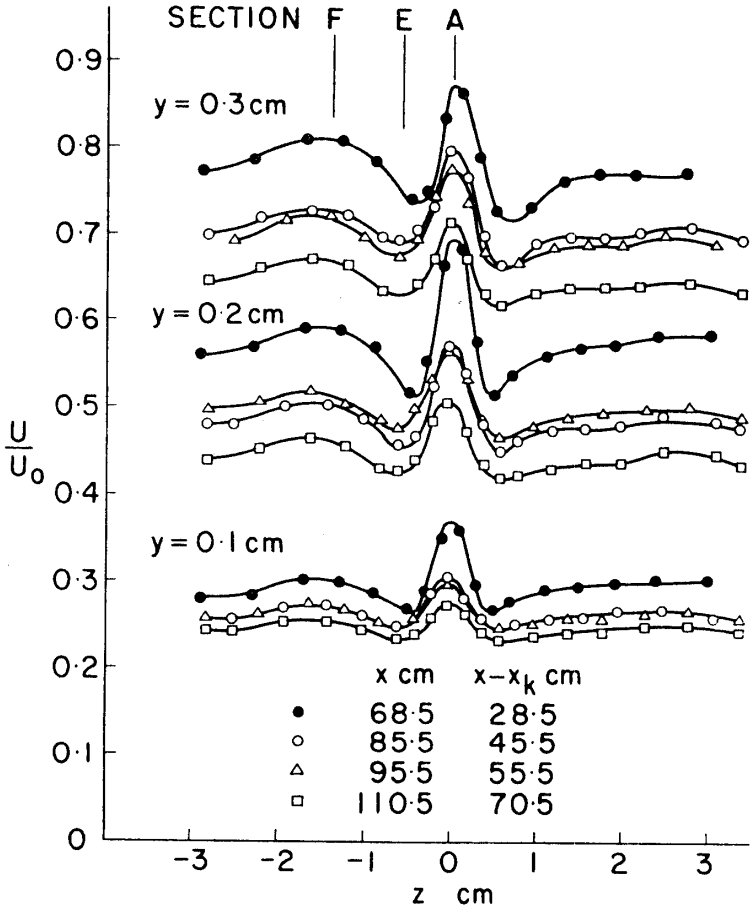

FIGURE 6. Spanwise distribution of mean velocity at a fixed height above flat plate at various distances from roughness element. Roughness height $k=0.2$cm, roughness location $x_k=40$ cm, free-stream velocity $U_0=6.6$ m/s, no current to vibrating ribbon. Wind tunnel LT-1.

Development of Controlled Disturbances

Controlled two-dimensional disturbances, or so-called Tollmien-Schlichting waves, were produced at a location $x_r = 75.5$ cm (35.5 cm downstream from roughness) by passing a current of a frequency of 45c/s through a phosphor-bronze ribbon, 0.03 mm thick, 4 mm wide and 30 cm long, spanned at a height of 0.67 mm from the plate, in the presence of a magnetic field. The Reynolds number, based on the free-stream velocity and boundary-layer displacement thickness, was 700, 920 and 850 in sections A, E and F, respectively, at the location of the vibrating ribbon, so that the exciting frequency of 45 c/s was the one to produce an amplifying Tollmien-Schlichting wave according to the two-dimensional small-perturbation stability theory.

When the current to the ribbon is weak, the rms wave intensity observed at downstream stations is in proportion to its initial value, or the current, indicating that the wave develops linearly. When the current exceeds a certain limit, however, the wave intensity is no longer proportional to the current, making the wave

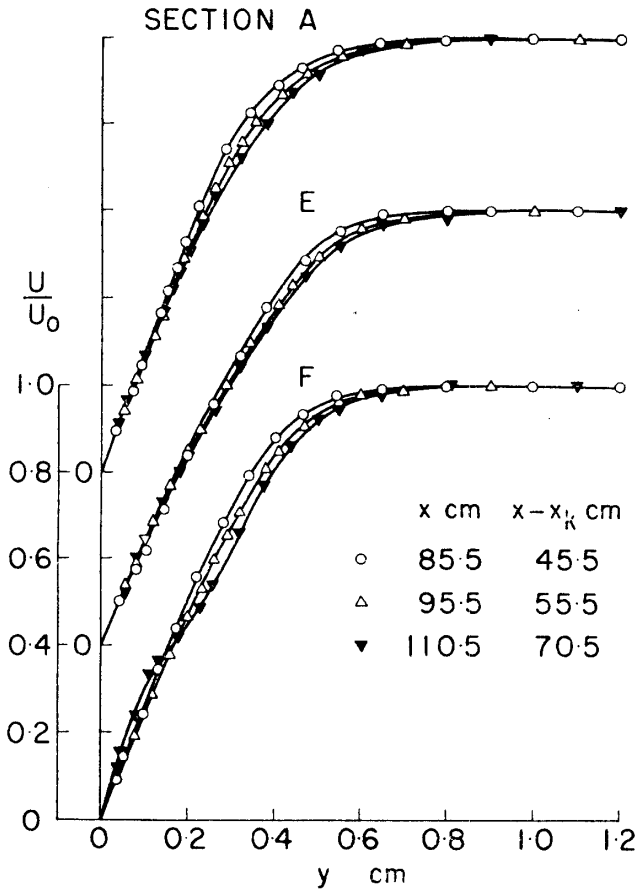

FIGURE 7. Distribution across boundary layer on a flat plate of mean velocity in sections A, E and F at various distances from roughness. Roughness height $k = 0.2$ cm, roughness location $x_k = 40$ cm, location of vibrating ribbon $x_r = 75.5$ cm, current to vibrating ribbon $i_r = 3$ amp. (nonlinear development), free-stream velocity $U_0 = 6.6$ m/s. Wind tunnel LT-1.

development nonlinear. So far as the wave development is linear, the distribution of mean velocity across the boundary layer does not change; it maintains the Blasius profile, which is observed when no current is passed through the vibrating ribbon. Distortion in mean velocity distribution appears only after the wave development becomes nonlinear. As seen from Figure 7, which shows the distribution of mean velocity in sections A, E and F at various downstream stations for nonlinear wave development, some distortion takes place in the course of downstream development, the distortion being most remarkable in section F.

Figures 8 and 9 show the spanwise distribution of rms wave intensity u_f at a frequency $f=45$ c/s at a fixed height above the plate at various distances $x-x_r$ from the vibrating ribbon for linear and nonlinear wave developments (current through ribbon 1 and 3 amp.), respectively. It is seen that the spanwise distribution of u_f is in phase with that of U (see Figure 6). It is moreover seen that the spanwise distribution of u_f maintains its shape in downstream development in the case of weak current, while the distribution is deformed in the case of strong current in such a way that a considerable amplification of wave intensity takes place in section F, while almost no amplification in section A.

Figures 10 and 11 show the distribution across the boundary layer of rms wave intensity u_f at a frequency $f=45$ c/s in sections A, E and F at various distances

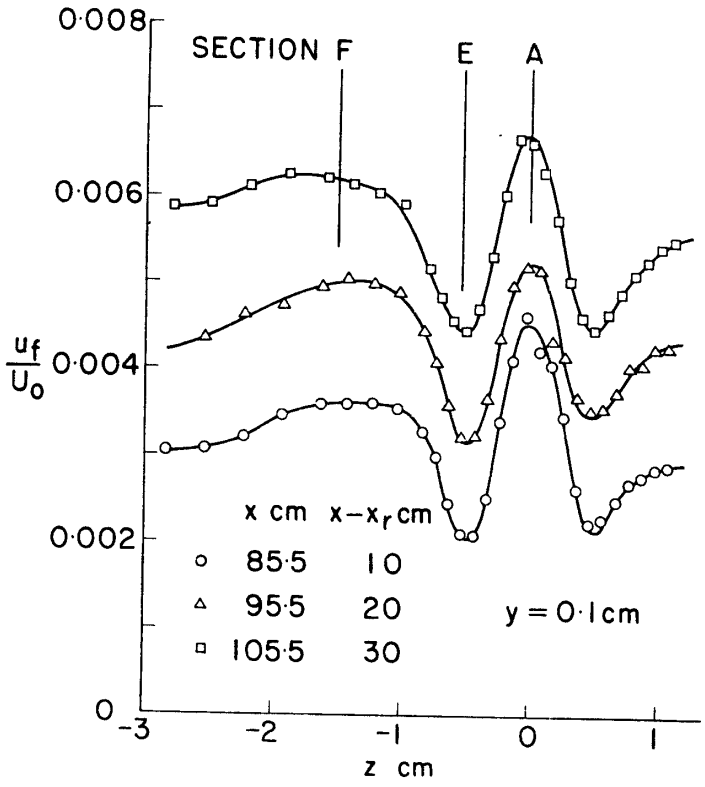

FIGURE 8. Spanwise distribution of rms wave intensity at a frequency of 45 c/s at a height of 0.1 cm above the flat plate at various distances from vibrating ribbon. Roughness height $k=0.2$ cm, roughness location $x_k=40$ cm, location of vibrating ribbon $x_r=75.5$ cm, current to vibrating ribbon $i_r=1$ amp. (linear development), free-stream velocity $U_0=6.6$ m/s. Wind tunnel LT-1.

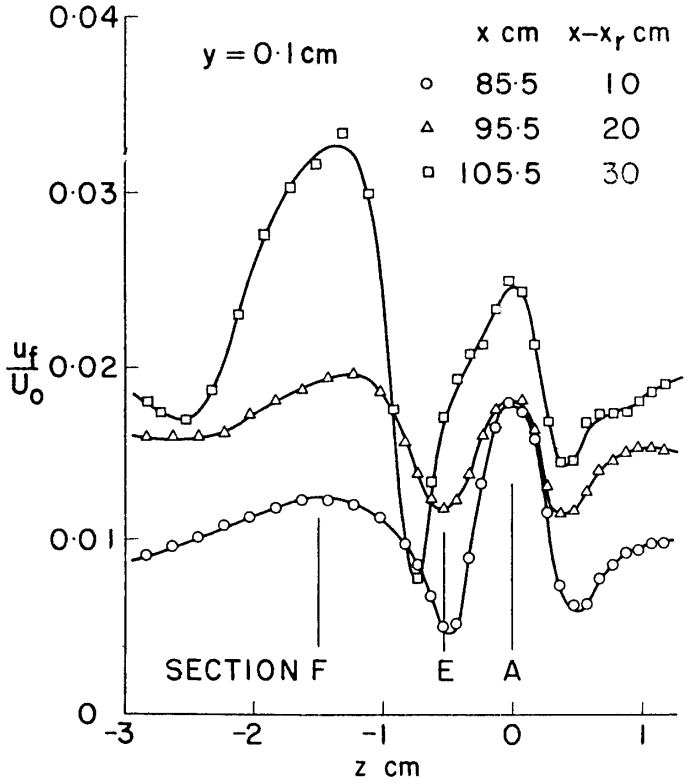

FIGURE 9. Spanwise distribution of rms wave intensity at a frequency of 45 c/s at a height of 0.1 cm above the flat plate at various distances from vibrating ribbon. Roughness height $k=0.2$cm, roughness location $x_k=40$cm, location of vibrating ribbon $x_r=75.5$ cm, current to vibrating ribbon $i_r=3$ amp. (nonlinear development), free-stream velocity $U_0=6.6$ m/s. Wind tunnel LT-1.

$x-x_r$ from the vibrating ribbon for linear and nonlinear wave developments, respectively. The abscissa is made non-dimensional by dividing the distance y by the boundary layer thickness δ defined as three times the displacement thickness for linear wave development. In linear wave development (Figure 10), the distribution of wave intensity in peak sections A and F are essentially of the type predicted by stability theory, accompanying a well-known phase shift of 180 degrees at a height of minimum intensity ($y/\delta=0.65$), while the distribution in valley section E is somewhat different and characterized by an M-shaped curve with a deep indentation at $y/\delta=0.17$, where an additional phase shift takes place. This disparity in intensity distribution is in general agreement with that observed by Tani and Komoda [*12*] on the boundary layer in the presence of streamwise vortices introduced by wings placed at regular intervals outside the boundary layer. In conformity with the indication of Figure 8, the maximum value of u_f increases downstream in all sections.

In nonlinear wave development (Figure 11), the wave is neither amplified nor damped in section A, until finally a change-over in distribution takes place to the M-shaped curve. In section E, the M-shaped distribution is maintained in the course of wave amplification, the peak closer to the wall becoming higher.

In section F, however, the wave is strikingly amplified, beyond comparison with other sections. The amplification is so rapid that a distortion takes place in

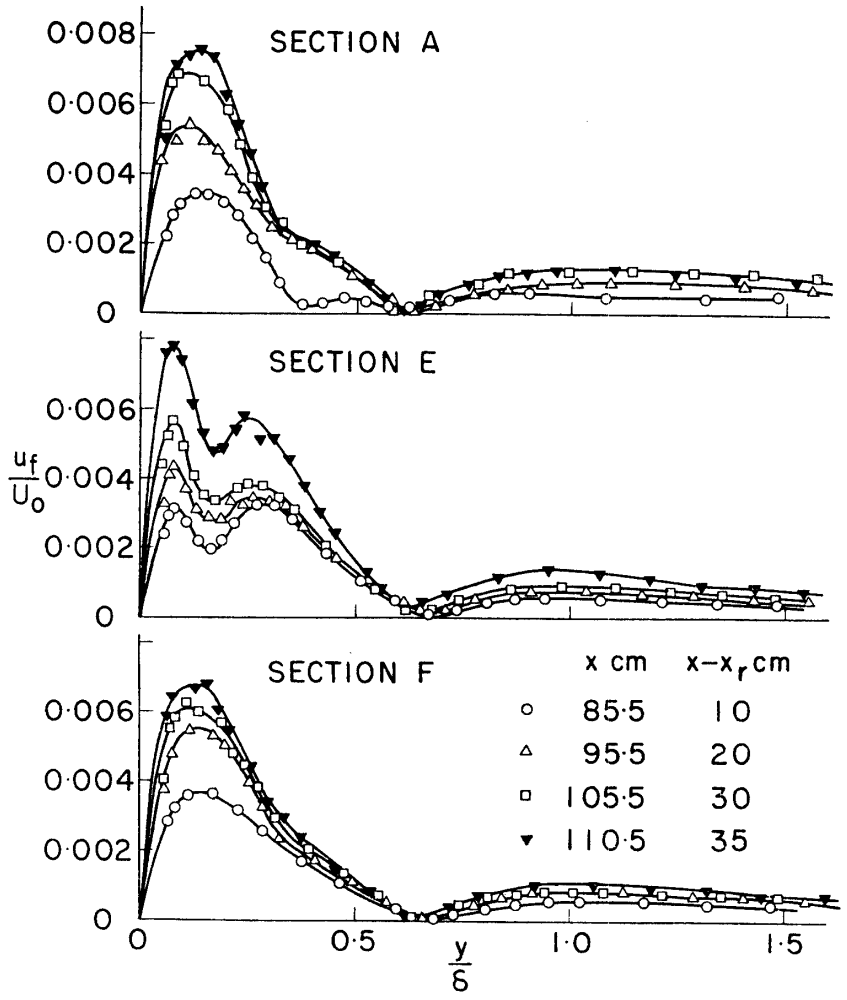

FIGURE 10. Distribution across boundary layer on a flat plate of rms wave intensity at a frequency of 45 c/s in sections A, E and F at various distances from vibrating ribbon. Roughness height $k=0.2$ cm, roughness location $x_k=40$ cm, location of vibrating ribbon $x_r=75.5$ cm, current to vibrating ribbon $i_r=1$ amp. (linear development), free-stream velocity $U_0=6.6$ m/s. Wind tunnel LT-1. δ is three times displacement thickness.

oscillograph wave form of velocity fluctuation in a layer close to the wall beginning from the station $x-x_r=30$ cm. This evolution corresponds to the distortion in mean velocity profile close to the wall as already mentioned in connection with Figure 7. At further downstream station $x-x_r=45$ cm, the oscillograph wave form is interspersed with spikes, characteristic of breakdown of laminar flow. This appears to explain why turbulence takes place in the form of a wedge, which originates from just outside of the horseshoe vortex.

CONCLUSION

Results of hot-wire measurements are presented on transition in laminar boundary layer along a flat plate with zero pressure gradient in the presence of an isolated roughness element. Transition occurs in the region of a wedge whose vertex moves

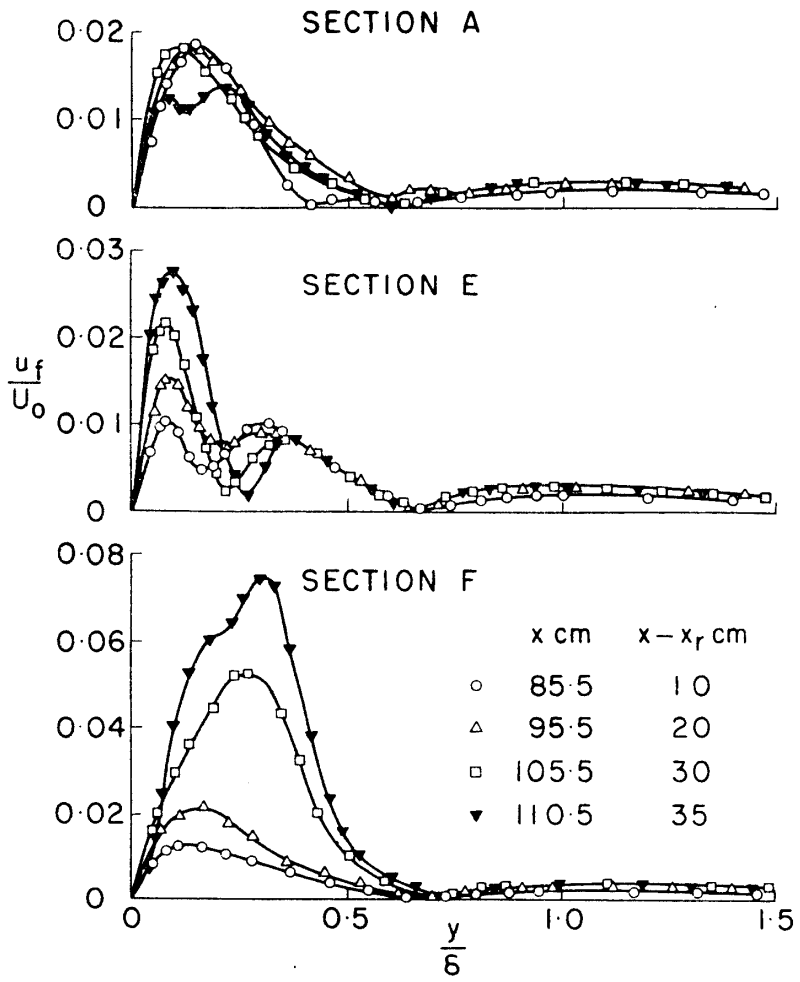

FIGURE 11. Distribution across boundary layer on a flat plate of rms wave intensity at a frequency of 45 c/s in sections A, E and F at various distances from vibrating ribbon. Roughness height $k=0.2$ cm, roughness location $x_k=40$ cm, location of vibrating ribbon $x_r=75.5$ cm, current to vibrating ribbon $i_r=3$ amp. (nonlinear development), free-stream velocity $U_0=6.6$ m/s. Wind tunnel LT-1. δ is three times displacement thickness for linear development.

rapidly forward with slightest increase in stream velocity or roughness height until finally it reaches the roughness element. The critical condition that just causes a wedge of turbulence to originate from roughness is governed by a critical value of the roughness Reynolds number R_k, which is based on the roughness height and the velocity in the laminar boundary layer at the height of roughness. The critical value of R_k is a slowly decreasing function of the transition Reynolds number R_t, based on the free-stream velocity and the distance from leading edge to roughness location.

The spanwise distribution of mean velocity in the boundary layer behind a roughness element for subcritical values of R_k is indicative of the presence of streamwise vortices as first observed by Gregory and Walker. Except for the station close behind roughness, a horseshoe-shaped vortex wrapped round the front of roughness gives a predominant effect on mean velocity distribution, producing a primary peak behind the centerline of roughness, and a valley and a secondary

peak outside. This three-dimensional deformation of mean velocity field is considered to account for the critical behavior of transition movement. Controlled two-dimensional disturbances created by a vibrating ribbon develop downstream in a way respectively characteristic of the central peak section, valley section and outside peak section. The disturbances are most strongly amplified in the outside peak section, until breakdown of laminar flow takes place at a downstream station. This breakdown corresponds to the beginning of a turbulent wedge at that station.

Department of Aerodynamics
Aeronautical Research Institute
University of Tokyo
September 10, 1962

References

[1] Gregory, N., and Walker, W. S.: The effect on transition of isolated surface excrescences in the boundary layer. ARC Tech. Rep. 13,436, 1950; published as ARC R. & M. No. 2779, 1956.

[2] Klanfer, L., and Owen, P. R.: The effect of isolated roughness on boundary layer transition. RAE Tech. Memo. No. Aero. 355, Mar. 1953.

[3] Fales, E. N.: A new laboratory technique for investigation of the origin of fluid turbulence. J. Franklin Inst., Vol. 259, pp. 491–515, 1955.

[4] Klebanoff, P. S., Schubauer, G. B., and Tidstrom, K. D.: Measurements of the effect of two-dimensional and three-dimensional roughness elements on boundary-layer transition. J. Aero. Sci., Vol. 22, pp. 803–804, 1955.

[5] Weske, J. R.: Experimental study of detail phenomena of transition in boundary layers. Tech. Note BN-91, Inst. Fluid Dyn. & Appl. Math., Univ. Maryland, Feb. 1957.

[6] Hama, F. R., Long, J. D., and Hegarty, J. C.: On transition from laminar to turbulent flow. J. Appl. Phys., Vol. 28, pp. 388–394, 1957.

[7] Schubauer, G. B.: Mechanism of transition at subsonic speeds. Grenzschichtforschung, Symposium Freiburg i. Br., August 1957, pp. 85–109; Springer-Verlag, 1958.

[8] Tani, I.: Effect of two-dimensional and isolated roughness on laminar flow. Boundary Layer and Flow Control, Vol. 2, pp. 637–656, Pergamon Press, 1961.

[9] Mochizuki, M.: Smoke observation on boundary layer transition caused by a spherical roughness element. J. Phys. Soc. Japan, Vol. 16, pp. 995–1008, 1961.

[10] Mochizuki, M.: Hot-wire investigations of smoke patterns caused by a spherical roughness element. Nat. Sci. Rep., Ochanomizu Univ., Vol. 12, pp. 87–101, 1961.

[11] Klebanoff, P. S., Tidstrom, K. D., and Sargent, L. M.: The three-dimensional nature of boundary-layer instability. J. Fluid Mech., Vol. 12, pp. 1–34, 1962.

[12] Tani, I., and Komoda, H.: Boundary-layer transition in the presence of streamwise vortices. J. Aerospace Sci., Vol. 29, pp. 440–444, 1962.

[13] Tani, I., and Sakagami, J.: Boundary layer instability at subsonic speeds. Paper presented at Third Congress ICAS, Stockholm, August 1962.

概　要

孤立した粗さによる境界層の遷移

谷　一郎・菰田廣之・小松安雄・井内松三郎

この報告は，圧力勾配のない平板に沿う層流境界層において，孤立した粗さにもとずく乱流への遷移の，熱線風速計による測定の結果をまとめたものである．遷移は楔形の領域でおこるが，楔の頂点は，流れの速度または粗さの高さの僅かの増加によって急激に前進し，ついに粗さの位置にまで到達する．この乱流の楔が，ちょうど粗さの位置から始まるようになるのは，'粗さレイノルズ数' R_k（粗さの高さおよび粗さの高さでの層流境界層の速度に関するレイノルズ数）がある臨界値を越えるときである．R_k の臨界値は，'遷移レイノルズ数' R_t（外側の流れの速度および平板前縁から粗さまでの距離に関するレイノルズ数）の増加とともに僅かに減少する．

粗さのうしろの境界層内の平均速度の横幅方向の分布は，Gregory と Walker によって始めて観察された，流れの方向に軸をもつ渦の存在を示している．粗さのすぐうしろの部分を除いて，平均速度の分布に主要な影響を与えるものは，粗さの前面にまきつく馬蹄形の渦であって，粗さの中心線上に速度分布の峰を生じ，さらにその外側に，それぞれ谷と第二の峰を生ずる．平均速度の場がこのように三次元的に変形することは，遷移点の前進が臨界的におこることに説明を与えるものと考えられる．細いリボンを振動させて，二次元的な攪乱を統制的に発生させると，その下流への発達は，中央の峰の断面，谷の断面，および外側の峰の断面において，それぞれ特徴的な過程をたどることがわかる．特に外側の峰の断面では，攪乱の増幅が極めて著しく，ついに下流の部分で，最初に層流の破壊を生ずるようになる．この破壊は，この断面から乱流の楔の始まることを示すものにほかならない．